Geophysical Journal International

Geophys. J. Int. (2016) **205,** 99–104
GJI Marine geosciences and applied geophysics

doi: 10.1093/gji/ggv528

Target-oriented Marchenko imaging of a North Sea field

Matteo Ravasi,[1,*] Ivan Vasconcelos,[2] Alexander Kritski,[3] Andrew Curtis,[4] Carlos Alberto da Costa Filho[4] and Giovanni Angelo Meles[4]

[1]*Statoil ASA, 5254 Bergen, Norway. E-mail: mrava@statoil.com*
[2]*Schlumberger Gould Research, Cambridge, CB3 0EL, United Kingdom*
[3]*Statoil ASA, 7053 Trondheim, Norway*
[4]*School of GeoSciences, The University of Edinburgh, Edinburg, EH9 3FE, United Kingdom*

Accepted 2015 December 9. Received 2015 December 8; in original form 2015 October 10

SUMMARY

Seismic imaging provides much of our information about the Earth's crustal structure. The principal source of imaging errors derives from simplicistically modeled predictions of the complex, scattered wavefields that interact with each subsurface point to be imaged. A new method of wavefield extrapolation based on inverse scattering theory produces accurate estimates of these subsurface scattered wavefields, while still using relatively little information about the Earth's properties. We use it for the first time to create real target-oriented seismic images of a North Sea field. We synthesize underside illumination from surface reflection data, and use it to reveal subsurface features that are not present in an image from conventional migration of surface data. To reconstruct underside reflections, we rely on the so-called downgoing focusing function, whose coda consists entirely of transmission-born multiple scattering. As such, we provide the first field data example of reconstructing underside reflections with contributions from transmitted multiples, without the need to first locate or image any reflectors in order to reconstruct multiple scattering effects.

Key words: Inverse theory; Interferometry; Body waves; Computational seismology; Wave propagation.

1 INTRODUCTION

Imaging the geometry and properties of complex subsurface geology, identifying and characterizing subsurface reservoirs of hydrocarbons, minerals or water, as well as monitoring of waste products stored underground such as CO_2 and nuclear waste, all require sophisticated seismic imaging and monitoring techniques. A crucial step for such imaging methods is the estimation of wavefields within the solid Earth's interior where no direct observations are available. Standard estimation or 'redatuming' approaches based on time-reversal of data recorded along an open boundary of surface receivers (Berryhill 1984) fail to explain how energy propagates in the complex subsurface unless high-resolution seismic velocity models are available *prior to* imaging, as otherwise they cannot accurately predict multiply scattered waves (multiples) in the subsurface. This causes large errors in images and, crucially, in interpretation.

Marchenko redatuming (or autofocusing) is a novel technique to estimate acoustic wavefields within the subsurface including primary and multiple reflections, using seismic waves measured at the Earth's surface and only a smooth estimate of the propagation velocity model (Rose 2002; Broggini *et al*. 2012; Wapenaar *et al*. 2013). Advantages over standard redatuming methods are that the multiply scattered wavefield coda is estimated at each subsurface image point, spurious arrivals due to multiples in the overburden are attenuated and the retrieved wavefields are naturally separated into their up- and downgoing components. The acoustic (fluid) Marchenko theory was extended to elastic (solid) media by da Costa *et al*. (2014), and by Wapenaar (2014), and by the elastic imaging of da Costa *et al*. (2015).

Standard migration techniques generate spurious structures in images as they do not correctly account for internal reflections. By contrast, Marchenko wavefields account for all multiples and Broggini *et al*. (2014) and Slob *et al*. (2014) construct images free from internal multiple artefacts by cross-correlating (or deconvolving) the retrieved up- and downgoing fields at any subsurface image point. Wapenaar *et al*. (2014) limit the computation of Marchenko fields to a single depth level, then use multidimensional deconvolution (Wapenaar *et al*. 2011) to create redatumed reflection responses from and to that depth, which are free of spurious events related to internal multiples in the overburden. These responses can be used for imaging target areas of the subusurface below or above the depth level of interest. Such images can be more accurate than

*Formerly at: School of GeoSciences, The University of Edinburgh, Edinburg, United Kingdom.

those generated by standard reverse-time redatuming followed by cross-correlation of the subsurface responses (Dong *et al*. 2009) as overburden multiples are removed.

This paper presents the first successful application of target-oriented imaging using Marchenko redatuming on real-field data. We apply the method to reflection seismic data recorded by an ocean-bottom cable (OBC) over the Volve oilfield, offshore Norway in 2002. One of the main obstacles to the application of such novel techniques to field data sets is the set of requirements for the reflection data (explained below). We show that a wave-equation method to redatum marine sources to the seabed, sea surface multiple removal and seismic source designature, transforms ocean-bottom data into a suitable estimate of the reflection response required by the Marchenko scheme. We then produce images of target areas of shallow and deep subsurface structures using Marchenko wavefields, and compare these to images obtained from standard reverse-time migration (RTM) of the same surface data.

2 MARCHENKO EQUATIONS

Marchenko redatuming is based on two wave states which uniquely relate subsurface wavefields from surface sources to so-called focusing functions via the recorded seismic data (Wapenaar *et al*. 2014). The subsurface wavefields ($\mathbf{g}^-$ and $\mathbf{g}^+$) belong to the wave state of the physical world in which data are acquired, while the focusing functions ($\mathbf{f}^-$ and $\mathbf{f}^+$) are defined in a modified medium that is homogeneous below a chosen subsurface level. These are related by (van der Neut *et al*. 2014)

$$\begin{aligned}\mathbf{g}^- &= \mathbf{R}\mathbf{f}^+ - \mathbf{f}^-\\ \mathbf{g}^{+*} &= -\mathbf{R}^*\mathbf{f}^- + \mathbf{f}^+\end{aligned} \tag{1}$$

Here $\mathbf{g}^-$ and $\mathbf{g}^+$ are matrices containing the time–space domain up- and downgoing Green's functions, with multiple sources at the acquisition surface and receivers located at a desired subsurface point. The focusing functions $\mathbf{f}^-$ and $\mathbf{f}^+$ are, respectively, up- and downgoing acausal solutions to the wave equation that focus at zero-time at the same subsurface point, and then continue as downgoing diverging fields into the homogeneous lower half-space. We suppose that $\mathbf{f}^+ = \mathbf{f}_\mathrm{d}{}^+ + \mathbf{f}_\mathrm{m}{}^+$, that is, $\mathbf{f}^+$ is composed of a direct wave $\mathbf{f}_\mathrm{d}{}^+$ followed by a coda $\mathbf{f}_\mathrm{m}{}^+$: these quantities are also organized in matrices with concatenated traces in the time–space domain. The operator $\mathbf{R}$ contains the real Earth's reflection response from vertical dipole sources to pressure receivers, and left multiplication is equivalent to performing multidimensional convolution in the time–space domain, while * acts on a matrix by time reversing its traces.

To obtain a system of coupled Marchenko equations, a muting function Θ that removes the direct arrival and all subsequent events is defined. Assuming that the muting function satisfies $\Theta\mathbf{g}^- = 0$, $\Theta\mathbf{g}^+ = 0$, $\Theta\mathbf{f}^+ = \mathbf{f}_m^+$ and $\Theta\mathbf{f}^- = \mathbf{f}^-$ (Wapenaar *et al*. 2014), its application to eq. (1) yields

$$\begin{aligned}\mathbf{f}^- &= \Theta\mathbf{R}\mathbf{f}_d^+ + \Theta\mathbf{R}\mathbf{f}_m^+\\ \mathbf{f}_m^+ &= \Theta\mathbf{R}^*\mathbf{f}^-.\end{aligned} \tag{2}$$

Starting from an initial focusing function $\mathbf{f}_\mathrm{d}{}^+$, obtained by inverting (or time-reversing) an estimate of the direct wave $\mathbf{G}_\mathrm{d}$ from the subsurface point to the surface and assuming a null coda ($\mathbf{f}_\mathrm{m}{}^+ = 0$), eq. (2) can be iterated to convergence. As noted by van der Neut *et al*. (2015) and Vasconcelos *et al*. (2015), the solution of the focusing functions at iteration K can be written in a compact form by means of a Neumann series expansion:

$$\begin{aligned}\mathbf{f}^{+(K)} &= \sum_{k=0}^{K}(\Theta\mathbf{R}^*\Theta\mathbf{R})^k\mathbf{f}_d^+\\ \mathbf{f}^{-(K)} &= \Theta\mathbf{R}\sum_{k=0}^{K}(\Theta\mathbf{R}^*\Theta\mathbf{R})^k\mathbf{f}_d^+.\end{aligned} \tag{3}$$

where each term in the series represents an update to the focusing function. Finally, up- and downgoing Green's function can be computed from eq. (1) using the estimated focusing functions $\mathbf{f}^-$ and $\mathbf{f}^+$.

3 MARCHENKO INPUTS AND REDATUMED FIELDS

Marchenko redatuming requires certain characteristics of the reflection response. $\mathbf{R}$ should be obtained from large aperture, fixed receiver arrays with dense source coverage coinciding with the entire receiver array, have broad bandwidth, and contain only primary reflections and internal multiples (i.e. be deprived of direct waves, ghosts and surface-related multiples). Recorded reflection data therefore approximate $\mathbf{R}$ only after pre-processing.

If data are acquired with standard ocean-bottom acquisition systems, wave equation approaches to joint source redatuming (to the receiver level), demultiple and source designature (Amundsen 2001) can transform recorded data into a suitable estimate of reflection response $\mathbf{R}$. These methods solve the following integral relation by means of multidimensional deconvolution (Wapenaar *et al*. 2011)

$$\mathbf{p}^- = \mathbf{R}\mathbf{p}^+ \tag{4}$$

where the recorded upgoing decomposed data ($\mathbf{p}^-$) is seen as the result of multidimensional convolution of the downgoing data ($\mathbf{p}^+$) and the desired reflection response ($\mathbf{R}$) that would be recorded in a hypothetical seismic experiment with no sea surface present. The decomposed data $\mathbf{p}^-$ and $\mathbf{p}^+$ are arranged in matrices containing responses from multiple sources to receivers at the acquisition surface. The sought reflection response $\mathbf{R}$ is also a matrix with responses from vertical dipole virtual sources to pressure receivers at the acquisition surface. Each frequency is inverted separately and the time–space response $\mathbf{R}$ is obtained by combining solutions of each inversion via an inverse Fourier transform.

For this study, we use data from an OBC on the seabed above the Volve field located in the gas/condensate-rich Sleipner area of the North Sea, offshore Norway. The receiver line contains 235 receivers spaced 25 m apart, and an overlying shot line of 241 sources spaced 50 m apart (Fig. 1(a)). Noise suppression, vector-fidelity corrections and initial source designature are applied to the data. Further, we scale the data by $\sqrt{t}$ to account for 3-D geometrical spreading and we calibrate the direct arrival of the particle velocity measurement to the pressure recording (see also Ravasi *et al*. 2015). After wavefield separation, the up- (Fig. 1b) and downgoing (Fig. 1c) components are used as input for multidimensional deconvolution (eq. 4), producing an estimate of the reflection response $\widehat{\mathbf{R}}$ for Marchenko redatuming (Fig. 1d). Standard RTM of $\widehat{\mathbf{R}}$ (i.e. the upgoing wavefield without source and receiver ghosts and free-surface multiples) is shown in Fig. 2 for comparison with Marchenko imaging.

An estimate of the direct wavefront $\mathbf{G}_\mathrm{d}$ is also required to create the initial focusing function $\mathbf{f}_\mathrm{d}{}^+$. We compute the traveltime of the first arriving wave from a subsurface point $\mathbf{x}_\mathrm{F} = \{6, 3.3\}$ km by ray tracing, then apply a 40 Hz Ricker wavelet with constant

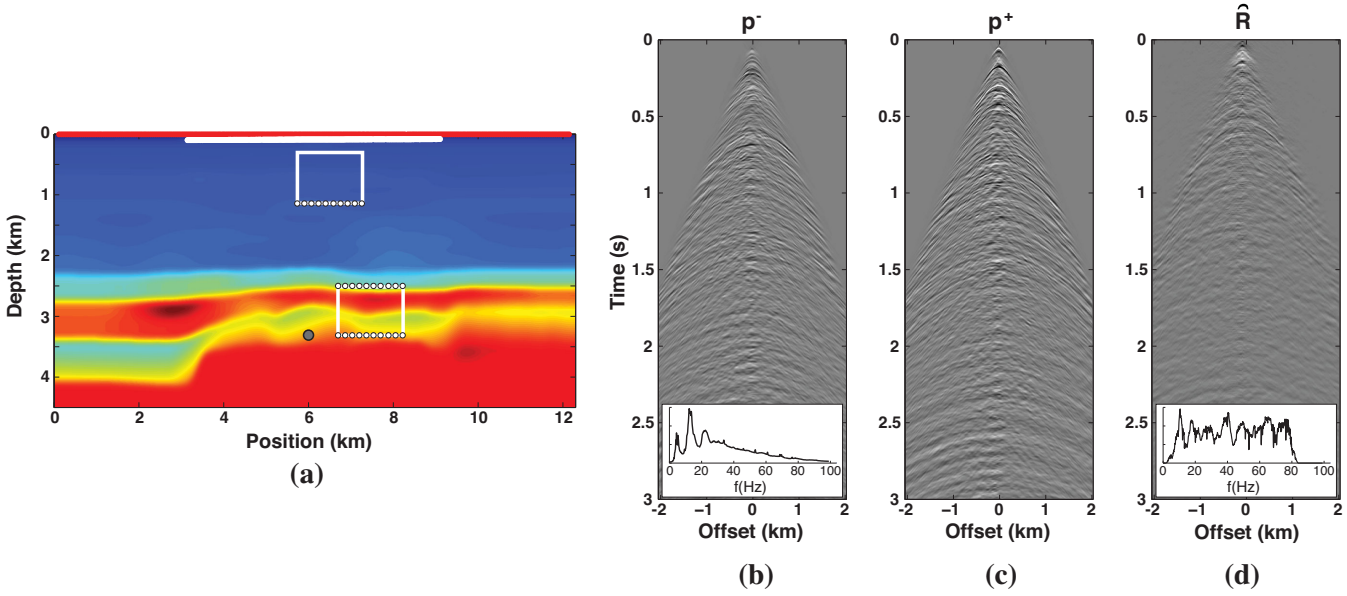

Figure 1. (a) Migration velocity model, source array at depth $z_S = 6$ m (red line) and receiver array at $z_R = 90$ m (white line) in the ocean-bottom cable acquisition. A grey dot represents the subsurface point where Marchenko fields shown in Fig. 3 are computed using eqs (1) and (3), while two white boxes indicate the target areas where Marchenko imaging is performed. Single common-shot gather of the (b) upgoing pressure data $\mathbf{p}^-$, (c) downgoing pressure data $\mathbf{p}^+$ and (d) estimate of the reflection response $\widehat{\mathbf{R}}$. Inserts in (b) and (d) show the average amplitude spectra of the gathers.

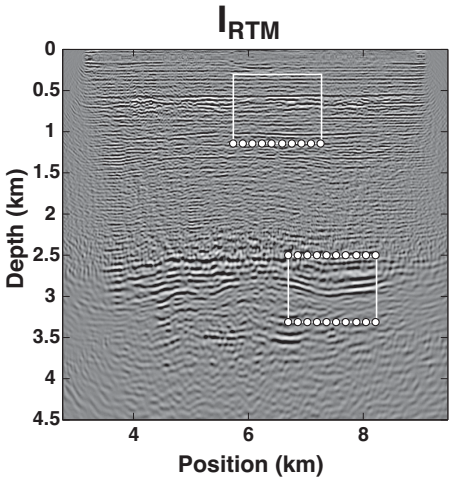

Figure 2. Subsurface image obtained by applying standard RTM to the estimate of the ideal reflection response ($\widehat{\mathbf{R}}$) shown in Fig. 1(d).

amplitude for all offsets (Fig. 3a). Focusing functions $\mathbf{f}^+$ and $\mathbf{f}^-$ estimated after two iterations of the Marchenko equations ($K = 2$ in eq. 3) are shown in Figs 3(b) and (c) and are used in eq. (1) to compute Green's functions $\mathbf{g}^+$ and $\mathbf{g}^-$ (Figs 3d and e). Note that the iterative Marchenko scheme has retrieved the coda in the downgoing field: a wave with similar moveout to the direct arrival is visible at zero-offset around 1.5 s in Fig. 3(d), which may have experienced multiple bounces in the high velocity layer in between 2.6 and 2.85 km depth.

A concern about the application of Marchenko redatuming to a field data is whether the iterative scheme presented above converges. Since we do not have direct access to the real Earth's reflection response $\mathbf{R}$, it is inevitable that the processed version of the recorded data $\widehat{\mathbf{R}}$ will be scaled, such that $\widehat{\mathbf{R}} = c_R\mathbf{R}$. Here, c_R is at best an unknown scalar (or, more likely, a compact filter varying in time and space) that depends on the acquisition and processing chain. In this application, we have taken advantage of the observation that $|(\Theta\widehat{\mathbf{R}}^*\Theta\widehat{\mathbf{R}})^k\mathbf{f}_d^+|^2 \rightarrow 0$ as $k \rightarrow \infty$ needs to hold for the Neumann series in eq. (3) to converge (see Supporting Material). While meeting this condition does not guarantee that each update has the correct amplitude and may not allow complete cancellation of spurious arrivals in the upgoing field, we show here that after two iterations of the Marchenko scheme this method produces a coda in the downgoing focusing function (Fig. 3b) and Green's function (Fig. 3d) with non-negligible amplitudes.

An accurate deconvolution of the source wavelet from the data is required for a correct summation of various updates of the Neumann series. In fact, each iteration of the Marchenko scheme involves one convolution and one correlation with reflection response $\widehat{\mathbf{R}}$ to obtain $\mathbf{f}^+$, and a further convolution to construct $\mathbf{f}^-$ (eq. 3): an unbalanced frequency response may enhance some frequencies relative to others, rendering the focusing function updates from different iterations incompatible. In this study, we mitigate the effect of the source signature from the data using the wave-equation demultiple approach of Amundsen (2001). While it is not possible to directly verify that the source wavelet has been fully deconvolved from the reflection data $\widehat{\mathbf{R}}$, we note that the original upgoing data show a much higher energy content at low frequencies (see insert in Fig. 1b) while the reflection response obtained from multidimensional deconvolution has a better equalized amplitude spectrum (see insert in Fig. 1d). However, since other factors such as frequency-dependent attenuation, imperfect deghosting, or noise affect the quality of the updates, an adaptive scheme may further improve the robustness of Marchenko redatuming (van der Neut *et al*. 2014).

4 MARCHENKO IMAGING

Marchenko redatuming produced up- and downgoing Green's functions for 151 subsurface points forming a 1.5 km wide array ranging from 6.7 to 8.2 km horizontally, at a depth of 2.5 km (lower

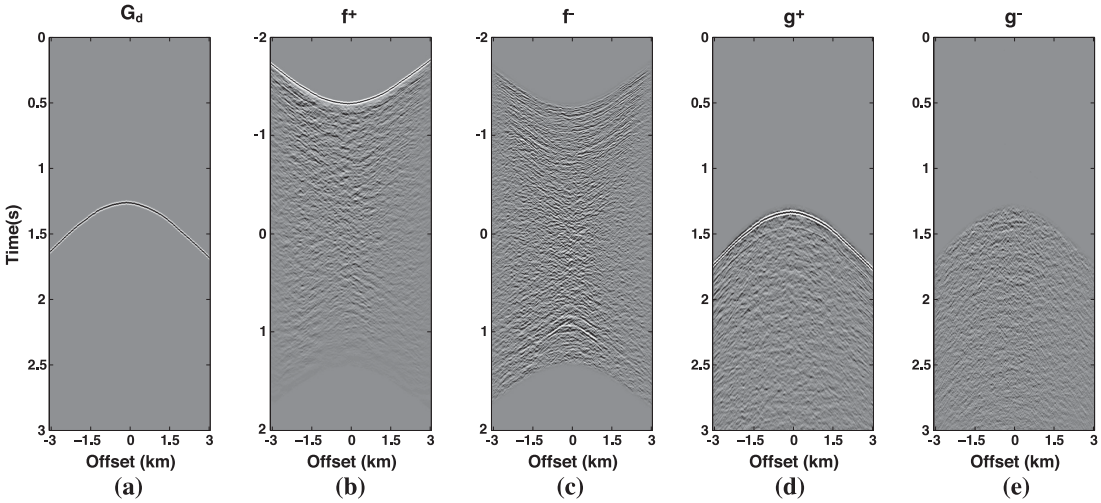

Figure 3. Marchenko redatuming. (a) Forward-modeled first arriving wave. (b) Down- and (c) upgoing focusing functions and (d) down- and (e) upgoing redatumed fields at $\mathbf{x}_F$. All panels are displayed with 50 per cent clipping of absolute amplitudes.

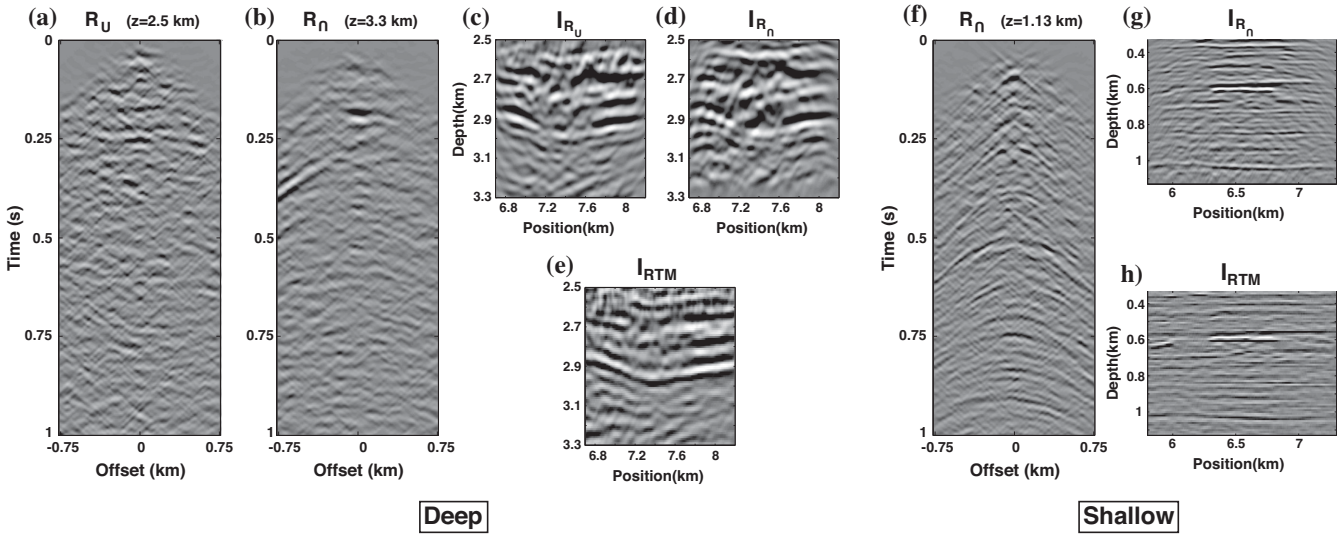

Figure 4. Marchenko imaging. Multidimensional deconvolution estimates of (a) reflection response from above $\mathbf{R}_\cup$ at depth level $z = 2.5$ km and (b) reflection response from below $\mathbf{R}_\cap$ at depth level $z = 3.3$ km. Images of the target zone from (c) above and (d) below, compared to that obtained from (e) standard RTM of the reflection response $\widehat{\mathbf{R}}$. (f), (g) and (h) are same as (b), (d) and (e) for a shallower depth level ($z = 1.13$ km).

target box in Fig. 1a). From these fields we obtain an estimate of the reflection response from above the target ($\mathbf{R}_\cup$) as if both sources and receiver were located along the array of subsurface points, within a modified medium with the same properties as the physical medium below the array but which is homogeneous above. We do so by solving the following equation by means of multidimensional deconvolution (Wapenaar *et al*. 2014):

$$\mathbf{g}^- = \mathbf{g}^+ \mathbf{R}_\cup. \tag{5}$$

The estimate of $\mathbf{R}_\cup$ for a source in the centre of the subsurface array is shown in Fig. 4(a). As discussed in Wapenaar *et al*. (2014), the redatumed reflection response can be used as input for standard imaging in a target zone just *below* the redatumed level (Fig. 4c). Comparison with standard RTM of our estimate of $\widehat{\mathbf{R}}$ shows that Marchenko imaging from above is able to produce an image comparable to that from RTM (Fig. 4e), perhaps improving details between the main reflectors at 2.6 and 2.9 km, and limiting the required (expensive) finite-difference computation for RTM to a smaller subsurface target zone.

The focusing functions $\mathbf{f}^-$ and $\mathbf{f}^+$ can also be combined to obtain a second estimate of the reflection response which illuminates the target area from below ($\mathbf{R}_\cap$) (Wapenaar *et al*. 2014):

$$-\mathbf{f}^{-*} = \mathbf{f}^+ \mathbf{R}_\cap. \tag{6}$$

The estimate of $\mathbf{R}_\cap$, shown in Fig. 4(b) for a source in the centre of the subsurface array at a depth of 3.3 km, is used to image the target zone just *above* the lower redatumed level (Fig. 4d) producing a similar image to panel c. Reflections $\mathbf{R}_\cap$ illuminating this portion of the subsurface from below contain complementary information to $\mathbf{R}_\cup$, at least when the lateral extension of the arrays of subsurface points used for imaging from above and below is the same. It is however important to note that the reflection $\mathbf{R}_\cap$ does not contain information from the portion of the subsurface below the focusing level: this is because $\mathbf{R}_\cap$ originates from focusing functions in a

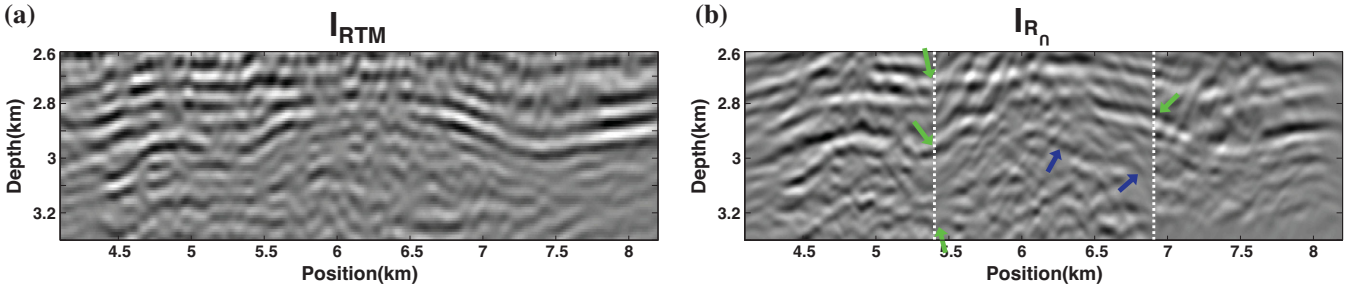

Figure 5. Merging of Marchenko images. (a) Standard RTM of the reflection response $\widehat{\mathbf{R}}$ and (b) Marchenko imaging from below of three different subsurface redatumed responses $\mathbf{R}_0$ (white dashed lines delimit the three images). Green arrows in (b) indicate near-perfect continuity between images. Blue arrows in (b) refer to a continuous structure revealed by Marchenko imaging that is not visible in the RTM image.

medium that is homogeneous below the focusing level (Wapenaar *et al*. 2014).

Similarly, Marchenko fields were computed along a line at 1.13 km depth (upper box in Fig. 1a) to image the complex stratigraphy in the shallow subsurface from below (Figs 4f and g). Spatial aliasing occurs in the standard RTM image (Fig. 4h) as this was originally sampled every 10 m to save on computational cost. The Marchenko image may be sampled relatively cheaply every 5 m due to the limited area of finite-difference modeling required, and compares favourably to that from RTM.

Marchenko imaging from below is performed for two additional subsurface lines with interreceiver spacing of 10 m: the first ranges from 5.4 to 6.9 km horizontally at depth 3.4 km, while the second is at 3.41 km depth and extends from 4.1 to 5.6 km horizontally. The resulting images are located either side of that in Fig. 4(d), and all three are merged to form Fig. 5(b). Note that since each of the reflection responses $\mathbf{R}_0$ is obtained using multidimensional deconvolution, the aperture of the subsurface array should not exceed that of sources at the acquisition surface for a successful inversion of eq. (6). Additionally, sparse (rather than dense) subsurface points will result in spatial aliasing, making the inversion unstable. With the choice of the extension and sampling of the subsurface array being limited by these constraints, it is important to assure that images obtained independently from different subsurface responses $\mathbf{R}_0$ at different depth levels show consistent structures. Green arrows in Fig. 5(b) indicate near-perfect continuity of reflectors between the various images, thus showing that we may design short-aperture, finely sampled subsurface arrays that prevent spatial aliasing in subsequent imaging. Finally, Marchenko imaging from below reveals structural features (blue arrows in Fig. 5b), which are not present in our surface RTM image of the reflection response $\widehat{\mathbf{R}}$ (Fig. 5a). While our interpretation of these events is that of physical structures that are perhaps hidden under coherent noise in the RTM image, they could also represent artificial structure arising from a suboptimal choice of the scaling c_R that overpredicts spurious events in the upgoing field (see Supporting Material).

5 CONCLUSIONS

The novel technique of Marchenko redatuming applied to an ocean-bottom seismic data acquired over the Volve North Sea field, produces encouraging results of target-oriented imaging of both shallow and deep structures. Although a by-product of the information contained in the original data, Marchenko focusing functions contain sufficient information to directly image the subsurface using reconstructed underside reflections. Such images reveal coherent features beneath strongly reflecting interfaces, which are distorted or invisible when imaging directly with surface data. This coherence supports the observation that the information in the retrieved focusing functions recasts that in the original data in a manner which is both nontrivial and useful. As such, we envisage that other practices that require wavefield focusing such as microseismic source localization, seismic time-lapse monitoring and non-destructive testing may also benefit from estimates of focusing functions from Marchenko redatuming.

ACKNOWLEDGEMENTS

The authors thank Edinburgh Interferometry Project (EIP) sponsors (ConocoPhillips, Schlumberger Cambridge Research, Statoil and Total) for supporting this research. We thank Statoil ASA, Statoil Volve team and Volve license partners ExxonMobil E&P Norway and Bayerngas Norge, for release of data and we are particularly grateful to G.R. Hall and H.A. Seter from the Statoil Volve team for help and support in seismic interpretation. Insightful inputs from L. Amundsen, K. Wapenaar and A. Ziolkowski, as well as the constructive comments of J. van der Neut and D.-J. van Manen are greatly appreciated.

REFERENCES

Amundsen, L., 2001. Elimination of free-surface related multiples without need of the source wavelet, *Geophysics,* **66**(1), 327–341.

Berryhill, J.R., 1984. Wave-equation datuming before stack, *Geophysics,* **49**(11), 2064–2066.

Broggini, F., Snieder, R. & Wapenaar, K., 2012. Focusing the wavefield inside an unknown 1D medium: beyond seismic interferometry, *Geophysics,* **77**(5), A25–A28.

Broggini, F., Snieder, R. & Wapenaar, K., 2014. Data-driven wavefield focusing and imaging with multidimensional deconvolution: numerical examples for reflection data with internal multiples, *Geophysics,* **79**(3), WA107–WA115.

Dong, S., Luo, Y., Xiao, X., Chavez-Perez, S. & Schuster, G.T., 2009. Fast 3D target-oriented reverse-time datuming, *Geophysics,* **74**(6), WCA141–WCA151.

da Costa Filho, C.A., Ravasi, M., Curtis, A. & Meles, G.A., 2014. Elastodynamic Green's function retrieval through single-sided marchenko inverse scattering, *Phys. Rev. Edit.,* **90,** 063201, doi:10.1103/PhysRevE.90.063201.

da Costa Filho, C.A., Ravasi, M. & Curtis, A., 2015. Elastic P and S wave autofocus imaging with primaries and internal multiples, *Geophysics,* **80**(5), S187–S202.

Ravasi, M., Vasconcelos, I., Curtis, A. & Kritski, A., 2015. Vector-acoustic reverse-time migration of Volve OBC dataset without up/down decomposed wavefields, *Geophysics,* **80**(4), S137–S150.

Rose, J.H., 2002. Single-sided autofocusing of sound in layered materials, *Inverse Probl*., **18,** 1923–1934.

Slob, E., Wapenaar, K., Broggini, F. & Snieder, R., 2014. Seismic reflector imaging using internal multiples with marchenko-type equations, *Geophysics,* **79**(2), S63–S76.

van der Neut, J., Wapenaar, K., Thorbecke, J. & Vasconcelos, I., 2014. Internal multiple suppression by adaptive Marchenko redatuming, in *84th Annual SEG Meeting,* Technical Program Expanded Abstracts, pp. 4055–4059.

van der Neut, J., Vasconcelos, I. & Wapenaar, K., 2015. On Green's function retrieval by iterative substitution of the coupled Marchenko equations, *Geophys. J. Int.,* **203,** 792–813.

Vasconcelos, I., Wapenaar, K., van der Neut, J., Thomson, C. & Ravasi, M., 2015. Using inverse transmission matrices for Marchenko redatuming in highly complex media, in *85th Annual SEG Meeting,* SEG Technical Program Expanded Abstracts, pp. 5081–5086.

Wapenaar, K., 2014. Single-sided Marchenko focusing of compressional and shear waves, *Phys. Rev. Edit.,* **90**(6), doi:10.1103/physreve.90.063202.

Wapenaar, K., van der Neut, J., Ruigrok, E., Draganov, D., Hunziker, J., Slob, E., Thorbecke, J. & Snieder, R., 2011. Seismic interferometry by crosscorrelation and by multi-dimensional deconvolution: a systematic comparison, *Geophys. J. Int.,* **185**(3), 1335–1364.

Wapenaar, K., Broggini, F., Slob, E. & Snieder, R., 2013. Three-dimensional single-sided Marchenko inverse scattering, data-driven focusing, Green's function retrieval, and their mutual relations, *Phys. Rev. Lett.,* **110**(8), 084301, doi:10.1103/PhysRevLett.110.084301.

Wapenaar, K., Thorbecke, J., van der Neut, J., Broggini, F., Slob, E. & Snieder, R., 2014. Marchenko imaging, *Geophysics,* **79,** WA39–WA57.

SUPPORTING INFORMATION

Additional Supporting Information may be found in the online version of this paper:

Figure S1. (a) Energy of $(\Theta\widehat{\mathbf{R}}^{*}\Theta\widehat{\mathbf{R}})^{k}\mathbf{f}_{d}^{+}$ (in logarithmic scale) versus number of iterations. (b) Energy of $\mathbf{g} + \mathbf{g}^{*}$ within the region where the window Θ equals one (in logarithmic scale) versus number of iterations. (http://gji.oxfordjournals.org/lookup/suppl/doi:10.1093/gji/ggv528/-/DC1).

Please note: Oxford University Press is not responsible for the content or functionality of any supporting materials supplied by the authors. Any queries (other than missing material) should be directed to the corresponding author for the paper.